The Effects of Backscattered Radiation into Beam Monitor Chamber: Study of 6 and 18 MV Conventional and Removed Flattening Filter Clinical Accelerator

Article *in* Biosciences Biotechnology Research Asia · April 2015

DOI: 10.13005/bbra/1601

4 authors, including:

Mansour Zabihzadeh
Ahvaz Jundishapur University of Medical Sciences. Ahvaz, Iran
83 PUBLICATIONS **193** CITATIONS
SEE PROFILE

Mohammad Reza Ay
Tehran University of Medical Sciences
183 PUBLICATIONS **1,392** CITATIONS
SEE PROFILE

Zahra Shakarami
9 PUBLICATIONS **9** CITATIONS
SEE PROFILE

BIOSCIENCES BIOTECHNOLOGY RESEARCH ASIA, March 2015. Vol. **12**(Spl. Edn. 1), p. 25-36

The Effects of Backscattered Radiation into Beam Monitor Chamber: Study of 6 and 18 MV Conventional and Removed Flattening Filter Clinical Accelerator

Mansour Zabihzadeh[1,2]*, Seyyed Rabi Mahdavi[3], Mohammad Reza Ay[4] and Zahra Shakarami[1]

[1]Department of Medical Physics, School of Medicine,
Ahvaz Jundishapur University of Medical Sciences, Ahvaz, Iran.
[2]Department of Radiotherapy and Radiation Oncology, Golestan Hospital,
Ahvaz Jundishapur University of Medical Sciences, Ahvaz, Iran.
[3]Department of Medical Physics, School of Medicine,
Iran University of Medical Sciences, Tehran, Iran.
[4]Department of Medical Physics and Biomedical Engineering,
School of Medicine, Tehran University of Medical Sciences, Tehran, Iran.

DOI: http://dx.doi.org/10.13005/bbra/1601

(Received: 05 February 2015; accepted: 10 March 2015)

In some linear accelerators (Linac), the collected charges in beam monitor chamber (BMC) is partly caused by the backscattered particles from the accelerator components downstream the BMC that influence the Linac output factors. In the intensity modulated radiation therapy technique, the desired dose distribution can be achieved through an unflattened beam. Although removing the flattening filter provides some advantages, the amount of backscatter radiation into BMC can be changed. In this study, contribution of backscattered particles into the BMC response of a Varian 2300 C/D Linac with and without a flattening filter was determined for 6, 18 MV photon beams. The experimental procedure included telescopic method and calculation procedure consisted of Monte Carlo simulation (MCNPX, version 2.4.0), were used to investigate the contribution of backscattered particles into the BMC performance. Our results showed a 2.3 % and 3 % increase in backscatter for a 0.5 × 0.5 cm² field compared to a 40 × 40 cm² field for 6 MV and 18 MV, respectively. The energy deposition from backscattered radiation is mainly caused by backscattered electrons. Removing the flattening filter did not change the BMC performance for a conventional Linac with a flattening filter. However, this result was not valid for small fields (e.g. 0.5 × 0.5 cm², 18 MV). The corrected backscatter factors is necessary to taking into account the contribution of backscattered radiation in the monitor chamber response for small fields in the case of the free flattening filter Linacs (18 MV).

Key words: Backscatter radiation, Flattening filter, Linac, MC simulation, Telescopic analysis.

In radiotherapy with linear accelerators (Linacs), the amount of delivered dose is measured by a beam monitor chamber (BMC) placed downstream of a beam flattening filter and upstream of beam collimating jaws. The interlock mechanism terminates the treatment as soon as the total charge collected by the chamber reaches a predefined monitor unit (MU) value set for each treatment. The dose measurement by BMC is expressed as monitor units (MUs). One MU is equal to 1cGy for a standard field size (10 × 10 cm^2) at a standard depth (10 cm) in a water phantom.

A fraction of transferred beam through the monitor chamber may be scattered backward from accelerator downstream components into the monitor chamber that can be re-read. In this

* To whom all correspondence should be addressed.
Tel: (+98)912-5032283; Fax: (+98)613-3332066;
E-mails: zabihzadeh@ajums.ac.ir

situation, the effects of backscattered radiation (photon and electron) shorten the switching-off time of radiation resulting in insufficient delivered dose to target volume queried number of MUs. This change on the turn-on time of beam influences the Linac output factor. Furthermore, using different collimating field sizes rather than the standard field changes the inside geometry of Linac head components. These factors can influence the amount of backscattered radiation into the BMC that lead to fluctuation in monitor chamber readouts. Therefore, changing the standard field size can change the ratio of delivered dose per MU.

The magnitude of the monitor backscatter (MBS) depends on the design of the monitor chambers, such as the thickness and material of the exit window and the distance from the chamber to the jaws. In addition, an anti-backscatter plate positioned downstream the monitor chamber can greatly reduce the size of the MBS effect[1].

The accuracy in monitor chamber readout is crucial to determine the accurate dose delivered to the patient. Therefore, considering appropriate correction factors for different field sizes because of different backscatter radiation into the monitor chamber is essential to derive an accurate dose to the target volume in treatment process.

Different methods such as photo activation[2], addition of an attenuator between the collimator and the monitor chamber[3] (inserting test objects into the Linac head), beam on time with beam current feedback disabled[4], number of beam pulses[5, 6], target charge integration[7-9] (changing the circuitry of the linac), and telescopic collimation[5, 8, 10-12] (making two thick and heavy collimators aligned on opening holes) have been used to measure the backscattering to the BMC of Linacs. These methods suffer some drawbacks such as invasiveness, dependence on the Linac stability, and invasive intervention to the Linac configuration and circuitry[2-12].

Previous studies have shown that backscatter radiation from the collimators is negligible for Varian accelerators such as the Linac 1800, possibly due to the thickness of the aluminum exit window on the BMC[7, 10], and the Linac 600 c because of a Mica chamber with copper plated stainless steel windows[12].

Yu *et al.* (1996)[5], Duzenli *et al.* (1993)[12] and Lam *et al.* (1998)[8] used the telescopic method to investigate the backscatter effect in the Varian 2100/2300 series Linacs. Their findings showed that the backscatter radiation towards the BMC influences the output factors of these series of Linacs. . For example, the results of Duzenli *et al.* (1993) study indicate a maximum 2.5% (6 MV) and 4% (18 MV) decrease in output for the Varian Linac 2100C[12].

The findings of the similar studies conducted by Lahan and Astruxton (1988) on the CGR Saturne 25 (23 MV), Patterson and Shragge (1981)[2], Kubo and Lo (1989)[11], and Kubo (1989)[10] on the AECL Therac-20 (18 MV) have shown that the chamber readouts can be affected by the backscattered particles into the BMC. For example, placing a 0.3 mm width copper foil above the flattening filter of the Therac-20 (18 MV) Linac at 0 × 0 cm^2 field size increased charge collection due to backscatter radiation by 10% compared with the 40 × 40 cm^2 field size[2]. Furthermore, some studies have reported that backscatter radiations influence the output factors of the Siemens Linac 6-15 MV[4, 13]. Analytical method was used to model the backscattering in monitor chamber[14]. In a study conducted by Verhaegen *et al.* (2000), both measurements with charge integration method and simulations (EGS4/BEAM) showed a linear increase in backscatter fraction with decreasing field size of the Varian 2100C Linac for photon (6 and 18 MV) and electron beams (6, 12, and 20 MeV) [9].

In the intensity modulated radiation therapy (IMRT) technique, dynamic multileaf collimator (MLC) positioning during irradiation could appropriately adjust the fluence distribution of an un-flattened beam to deliver a desired uniform or non-uniform dose distribution. Therefore, the flatness of initial radiation distribution produced by flattening filter across the beam is unnecessary in this method. According to the previous studies, removing the flattening filter has some advantages such as reduced treatment time through higher fluences and dose rates, smaller out-of-field dose for patients due to reduced head-leakage dose, lower head scatter and smaller leakage dose through the MLC[15-20]. Although the effect of backscatter radiation on the BMC readout is well

known for conventional machines (like Varian linac 2100C with a Kapton monitor chamber), the possible effects have not been investigated in free flattening filter mode.

In this study, the backscatter radiation into the BMC was measured using telescopic method for the flattening filter in place (FF mode). These data were compared with the published data to validate our proposed simulated model. In addition to the standard FF mode of Varian Linac (6MV and 18 MV), we calculated the amount of backscatter radiation from different field sizes on BMC readout without flattening filter (free flattening filter, (FFF mode)). Furthermore, spectra of forward directed and backscattered particles into the BMC were calculated for both conditions**.**

MATERIALS AND METHODS

Measurement Procedure

All dose measurements including depth dose curves and dose profiles were carried out using a PTW- MP2 scanner with an ionization chamber at the water phantom ($50 \times 50 \times 50$ cm^3). The cylindrical chamber has an inner diameter of 6 mm and the effective measurement point was 0.6 r_{inner} (where r_{inner} is the radius of the chamber cavity) upstream of the chamber center, consistent with the AAPM TG-51 protocol[21]. The scanning system has a position accuracy of d" 1 mm and a reproducibility level of d" 0.1 mm.

In this study, we used a simple telescopic method to measure the backscatter radiation contribution into the BMC. The measurements' set up is shown in Figure 1.

The concept of the telescopic method is based on preventing the scattered radiation generated in a flattening filter, ring shields and collimators to reaching the ionization chamber located behind the second slit[5, 8, 10-12]. Therefore, it is expected that the telescopic measurements should yield a constant output, assuring that the applied telescope eliminates the contribution from forward scattering. For this, to collimate the directed vertically X-ray beam towards the floor, a pair of 7.6 cm thickness slits with a central aperture of 3 mm-radius was made of Cerrobend. The first slit (upper slit) was positioned immediately behind the lower (x) jaws on the accessory mount at the distance of 64.8 cm from the target. The second slit was positioned on Styrofoam stand at distance of 200 cm from the target and its radius determines the field of view for scattered radiation. An ionization chamber, IC-1, (0.6 cc Farmer type, PTW model, Freiburg) with proper buildup cap (1mm and 4mm brass thickness for 6 MV and 18 MV, respectively) was positioned horizontally behind the lower slit to record the charges while surrounded by jaws. The holes in the Cerrobend slit and the sensitive volume of the chamber were aligned with the central axis of the beam by the cross hair of the light field and laser. Because the

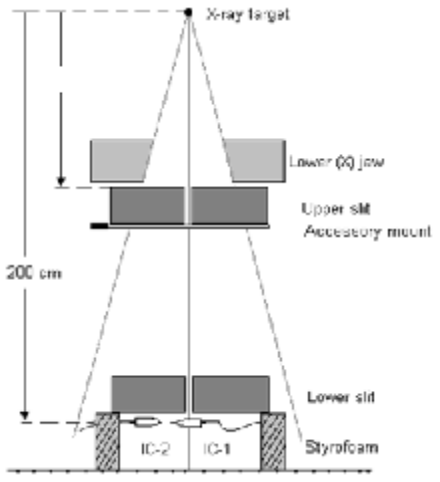

Fig. 1. Measurement setup for a narrow beam telescopic method using two ionization chambers and two pin-hole blocks of cerrobend and lead.

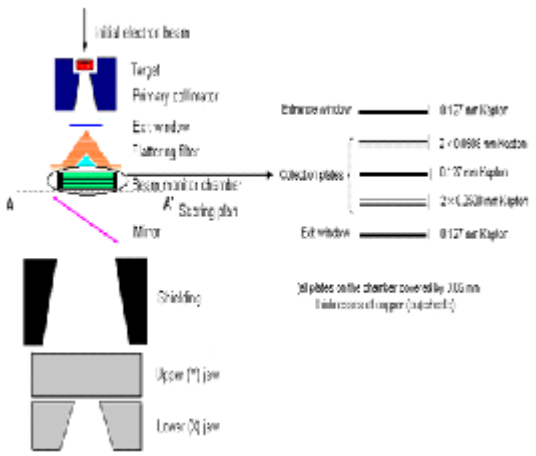

Fig. 2. Schematic diagram of the MC model for the Varian 2300C/D (18 MeV) linac geometry. Surface-Source files are scored at the level AA'.

change in reading of IC-1 for different field sizes setting is small, the change in scattered radiation can be significant. To consider remained scattered and stray photons that can be contributed the chamber reading; another similar ionization chamber (IC-2) was positioned away from central beam axis and next to the IC-1. During each square field size (ranged from 0.5 × 0.5 up to 40 × 40 cm^2) reading, the contributions from the scattered and stray photons for IC-2 were subtracted from the reading of IC-2. Same time reading of IC-1 and IC-2 removes the set up errors. Reading of chamber to collect charges was recorded for 500 MU and was repeated 3 times for each field size.

Monte Carlo Simulation study

The Monte Carlo code MCNPX version 2.4.0 was used to model photon beams form the Varian 2300C/D Linac for 6 and 18 MV[22]. MCNPX is a well-known general-purpose Monte Carlo code developed at Los Alamos National Laboratories that extends the transport capability of MCNP in order to include 34 particles over a more complete energy range. Using the tabulated interaction cross sections for most neutral and charged particles (<150 MeV) radiation transport of these particles can be simulated in radiation therapy applications. Figure 2 shows the schematic diagram of the simulated geometry for the Varian 2300C/D Linac. The right half of the Figure 2 shows the true geometry of the Linac chamber. The definitions of window and collection plate materials and thicknesses of the monitor chamber were as per the study of Duzenli *et al.* (1993)[23] and the Monte Carlo project prepared by manufacturer.

The model included the bremsstrahlung target, the primary collimator, vacuum window, the flattening filter, the monitor ion chamber, the mirror, the shielding rings, and the upper and lower jaws.

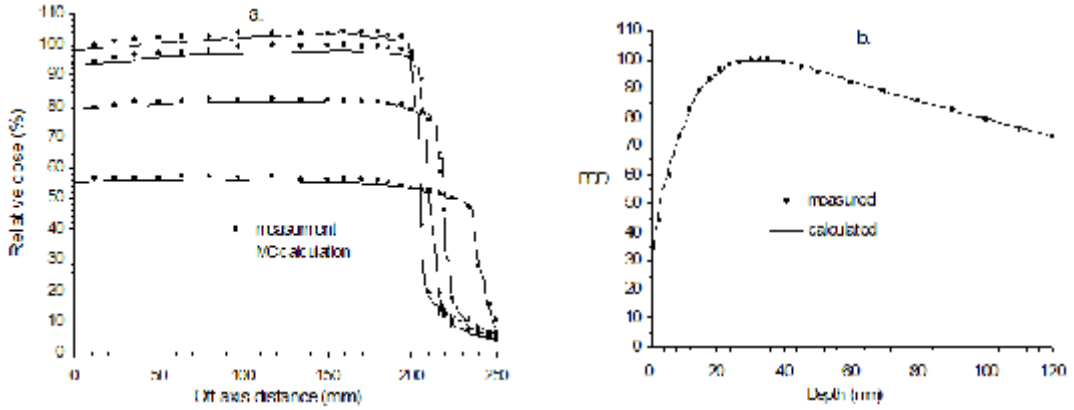

Fig. 3. Comparison of the Monte Carlo calculations with water phantom measurements: a. dose profiles at depths of 3, 5, 10 and 20 cm for the 40 × 40 cm^2 field size, b. PDD curve for the 10 × 10 cm^2 field size.

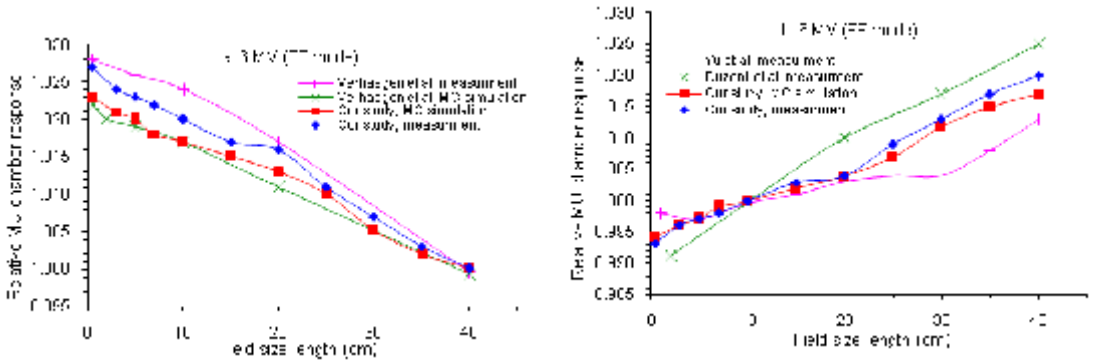

Fig. 4. The variation of relative BMC response as a function of field size for 6 MV photon beam of the conventional Linac (FF mode). All data are normalized to a) the 40 × 40 cm^2 field size, b) the 10 × 10 cm^2 field size.

All of the models in this study especially the BMC were accurately and carefully built using the composition and geometry of this Linac components provided by manufacturer. The distance between the downstream surface of the BMC and the top of the closed upper jaws is 11.5 cm in our Varian 2300C/D linac. The exact mean energy of the electron beam incident on the target may depart from a nominal potential that is not accurately known. Therefore, electron energies should be tuned through repeated calculations until a reasonably well agreement between the measured and simulated values of the depth doses and dose profiles were reached.

The final incident electrons had a Gaussian energy distribution with a full width of half maximum (FWHM) of 1 MeV that was centered at 6 MeV and 18.2 MeV for 6 MV and 18 MV, respectively. The electron beam radial intensity distribution was also set to a Gaussian with the FWHM of 1.1 mm and 1.4 mm for 6 MV and 18 MV, respectively. Inside the phantom, to calculate the depth doses and dose profiles, the cut-off energy was determined as 0.01 and 0.521 MeV for the photons and electrons, respectively. For depth dose calculations within the water phantom, a cylinder with a radius of one-tenth the size of the open field size was defined and divided into scoring cells with 2 mm height along the beam central axis. For beam profile calculations, the primary cylinder was positioned at the predefined depth vertically to the beam central axis with the radius of 2 mm. Therefore, the dose resolution was 2 mm in this study. The F6: E tally was used for dose calculations in the water phantom.

In our simulation the deposited energy in the air of chamber is calculated based on the assumption that this quantity is linearly related to the collected charge from the chamber[9]. The dose distribution from photons (including secondary

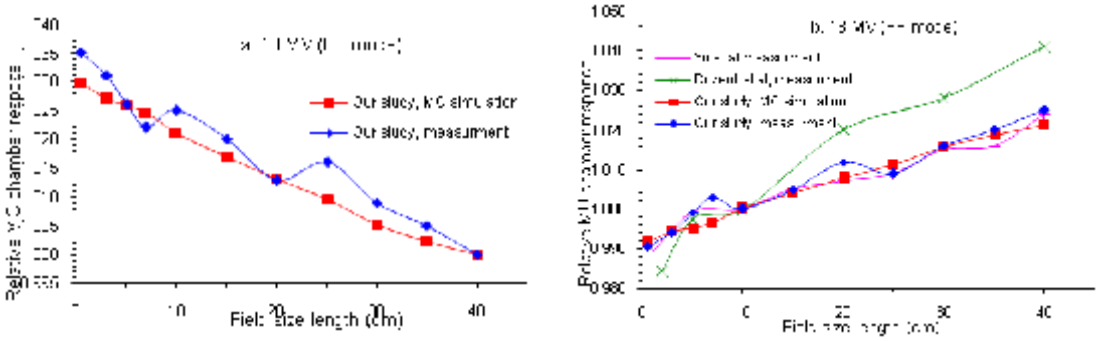

Fig. 5. The variation of relative BMC response as a function of field size for 18 MV photon beam of the conventional Clinac (FF mode). All data are normalized to a. the 40 × 40 cm^2 field size, b. the 10 × 10 cm^2 field size.

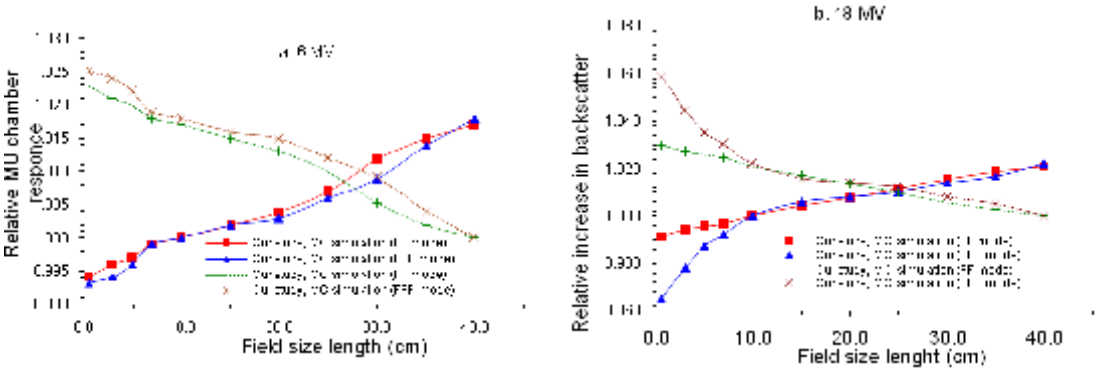

Fig. 6. Relative increase in backscatter into MU chamber (two lower curves, normalized to 10 × 10 cm^2 field size) and relative increase in backscatter (two upper curves, normalized to 40 × 40 cm^2 field size); a. for 6 MV, b. for 18 MV.

electrons and electron contamination) in the chamber is calculated using the F6 tally (in units of MeV/g) for electrons (F6: E) since photons transfer all their energy to electrons in photo-atomic interactions. The F6: E tally is a new feature of MCNPX that is a track-length estimator for charged particles based on the restricted or total stopping power of the particle[22]. In the first step of our simulation, we considered a scoring plan with opposite sign to the beam transferring immediately at downstream surface of the chamber (AA' in Fig. 2). All applied square field sizes (ranged 0.5 × 0.5 to 40 × 40 cm^2) were defined at 100 cm distance from the target. The total deposited energy in the chamber was scored and the spectra of the forward directed photons and electrons on the upper surface of BMC were separately obtained. Using the phase space file the spectra of the backscattered photons and electrons were calculated separately and the total deposited energy from backscattered particles was scored.

In the next step, rewriting the program by using the PTY parameter (PTY E), only the contribution of penetrated electrons from downstream components of Linac into the BMC were calculated. The maximum flounce for the forward directed photons was normalized to unity.

To reduce computing time and for acceptable statistical uncertainties, different importance values as particle splitting were considered for components of our model. The greatest importance, 40, was chosen for air of the

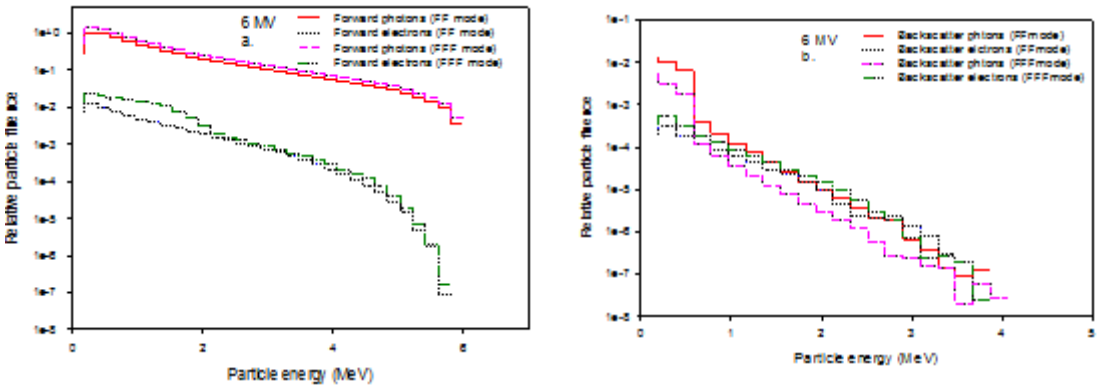

Fig. 7. The fluence spectra of 6 MV reached to the upstream surface of the BMC in the case of the FF and FFF mode, a. for the forward directed photons and electrons for each field size, b. for the backscattered photons and electrons for the 0.5 × 0.5 cm^2 field size. The spectra have been normalized to the maximum of the forward photon fluence in the case of the FF mode for the 0.5 × 0.5 cm^2 field size.

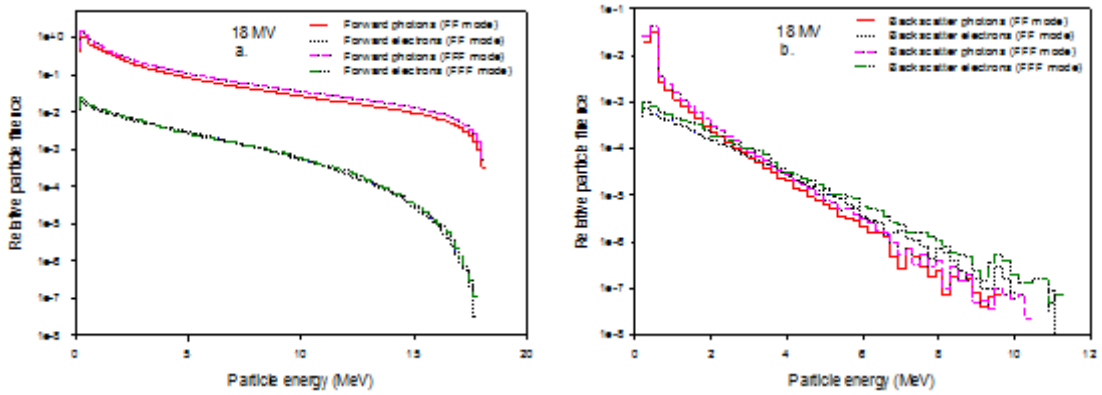

Fig. 8. The fluence spectra of 18 MV reached to the upstream surface of the BMC in the case of the FF and FFF mode, a. for the forward directed photons and electrons for each field size, b. for the backscattered photons and electrons for the 0.5 × 0.5 cm^2 field size. The spectra have been normalized to the maximum of the forward photon fluence in the case of the FF mode for the 0.5 × 0.5 cm^2 field size.

chamber where increasing distance from chamber decreases importance value.

The backscattered particle spectrum extends down to low energies. To calculate the contribution of deposited energy from these low energy particles in the air part of the monitor chamber, the transport cut-off energies of 0.1 MeV and 0.01 MeV were respectively considered for electron and photon transporting for the Linac head components.

To benchmark the model with the flattening filter, the simulated data were compared with the published data reported by Yu *et al.* (1996) that the amount of backscatter from collimators to the BMC measured as current pulses per MU. Therefore, the simulated energy deposition per incident particle was converted to particles per energy deposition and normalized to the 10 × 10 cm^2 field size. Any detection efficiency was not considered to MC results.

RESULTS AND DISCUSSION

The MC-calculated PDD (percentage depth dose) curves and beam profiles were firstly compared with the measurements, to validate our MC model. There was a good agreement between the measurements and calculations for beam profiles and PDD curves (Figure 3). Local differences of less than 1 % were seen for PDD values in descending part up to 30-cm depth, but it increased up to 6 % for the buildup region and for the largest field size; e.g. 40 × 40 cm^2 (Fig. 3a). The discrepancies of about 5% were observed by Ding (2002) in the buildup region for the field with the lead foil between calculated dose by Monte Carlo and measurements[24]. For smaller depths and small field sizes, the Monte Carlo simulations overestimated the dose in the buildup region while for larger field sizes they underestimated the dose [15, 25]. Hartmann Siantar *et al.* (2001) suggested that this discrepancy was caused by a source of electrons in the linac head that was not considered for Monte Carlo simulation of the head[26]. On the other hand, a study by Ding (2002) showed that this discrepancy is not due to the electron contaminant[24]. The amount of neutron dose in a high-energy photon beam reported by Nath *et al.* (1984) is too small to explain these discrepancies [27]. For beam profiles, local differences less than 2 % were seen for flat region, but it increased to 13 % for region located out of field (figure 3b).

The effect of backscattered particles on the BMC response for conventional Linac (FF mode)

The backscatter effect on the BMC response as a function of field size was investigated by measurement and simulation methods. The contribution of the backscatter radiation in the BMC from telescopic measurements and simulations are shown in the Figs. 4a and 4b for 6 MV and in the Figs. 5a and 5b for 18 MV photon beam.

The maximum IC-2 reading to considering scattered and tray photons into IC-1 response increased as field size increased that was approximately 0.5%. The contributions by the scattered and stray photons were subtracted from the chamber readings in data analysis. This small value also indicates that our setup properly prevents reaching of scatter and tray photons to the IC-1. The measurement uncertainty is of the order of 1%. The calculated uncertainties in total energy deposition into the chamber air volume for 6 MV ranged 0.22 % at 0.5 × 05 cm^2 to 0.24 % at 40 × 40 cm^2. The related uncertainties of deposited energy from the total backscatter radiation contribution ranged 1.3 % to 1.5 %. Decreasing square field sizes increased the contribution of the backscatter radiation into the BMC in an almost linear manner (Fig. 3a). The increase of backscatter fraction for a 0.5 × 0.5 cm^2 field, compared with a 40 × 40 cm^2 was respectively 2.7 % and 2.3 % for the measured and simulated data (Fig. 4a). The corresponding increase from the reported data by Verhaegen *et al.* (2000) was 2.85 % and 2.25 %[9]. Verhaegen *et al.* (2000) reported the measurement uncertainty as the order of 1%[9], while the calculated uncertainty was usually less than 0.5 %. In addition, our data for 6 MV are compared with the measured data reported by Yu *et al.* (1996) [5] and Duzenli *et al.* (1993)[12] (Fig. 3b). The absolute uncertainty of Yu *et al.* (1996) data was 0.4 %[5] and Duzenli *et al.* (1993) did not report any uncertainty[12]. Our data are in good agreement with the results of Ye *et al.* (1996)[5] and Verhaegen *et al.* (2000)[9] studies and located within the given statistical uncertainties (see Figs. 3a and 3b). However, our data are not in good agreement with the data reported by Duzenli *et al.* (1993)[12] (Fig. 3b). As mentioned earlier, Duzenli *et al.* (1993) did

Table 1. The mean energy and total fluence of forward and backscattered photons and electrons for 0.5 × 0.5 cm^2 and 40 × 40 cm^2 field size for 6 MV and 18 MV photon beam. The mean statistical uncertainties of the total fluences included in parenthesis.

Field size		0.5 × 0.5 cm^2				40 × 40 cm^2			
		Mean energy		Total fluence		Mean energy		Total fluence	
		6 MV	18V	6 MV	18 MV	6 MV	18 MV	6 MV	18 MV
Backscattered photons	FF mode	0.36	0.53	3.00×10^{-7} (0.33 %)	3.26×10^{-6} (0.15 %)	0.30	0.38	1.65×10^{-7} (0.42 %)	1.07×10^{-6} (0.25 %)
	FFF mode	0.34	0.52	4.59×10^{-7} (0.46 %)	4.50×10^{-6} (0.24 %)	0.28	0.36	2.42×10^{-7} (0.49 %)	1.34×10^{-6} (0.42 %)
Backscattered electrons	FF mode	0.68	1.33	1.07×10^{-8} (1.76 %)	2.06×10^{-7} (0.87 %)	0.47	0.95	5.13×10^{-9} (1.81 %)	6.34×10^{-8} (0.89 %)
	FFF mode	0.64	1.32	1.73×10^{-8} (2.24 %)	2.85×10^{-7} (2.11%)	0.47	0.89	1.01×10^{-8} (5.03 %)	7.79×10^{-8} (2.93%)

		Each field size			
		Mean energy		Total fluence	
		6 MV	18 MV	6 MV	18 MV
Forward photons	FF mode	1.39	2.97	6.58×10^{-5} (0.12 %)	4.34×10^{-4} (0.03 %)
	FFF mode	1.35	2.74	8.89×10^{-5} (0.11 %)	5.21×10^{-4} (0.03 %)
Forward electrons	FF mode	1.08	2.96	6.85×10^{-7} (0.27 %)	9.81×10^{-6} (0.14 %)
	FFF mode	1.06	2.85	1.48×10^{-6} (0.57 %)	1.08×10^{-5} (0.43 %)

not report statistical uncertainties, but considering an uncertainty of 1 %, reported by Verhaegen *et al.* (2000)[9], our data are in good accordance with the data of Dunzeli *et al.* (1993)[12].

Results of 18 MV photon beam for conventional Linac (FF mode) are presented in Figs. 5a and 5b. The statistical uncertainties in the total energy deposition for the simulated 18 MV photon beam ranged 0.12 % at 0.5 × 0.5 cm^2 to 0.13 % at 40 × 40 cm^2. The corresponding statistical uncertainty in energy deposition from the backscattered particles ranged 0.69 % to 0.73 %. For 18 MV photon beam (FF mode), the maximum increase in backscatter fraction for a 0.5 × 0.5 cm^2 field, compared with a 40 × 40 cm^2 was 3.5 % and 3 % for our measured and simulated data, respectively (Fig. 5a). Our measured and calculated results for 18 MV were in relative agreement with the data of Yu *et al.* (1996)[5], whereas no agreement with the data of Duzenli et al. (1993)[12]. Our calculated and measured data were closely matched with the published data by Yu *et al.* (1996)[5] and were of the same uncertainties reported by Duzenli *et al.* (1993) [12]. For 18 MV photon beam, similar to 6 MV, decreasing the field size will increase the backscatter radiation into the BMC. The increased backscatter radiation will reduce the amount of primary radiation reached to the chamber and switch off the beam earlier.

In general, our calculated and measured data for the backscatter contribution (Figs 4 and 5) due to the field size change are in good agreement within statistical uncertainty; however, there are small systematic differences between our calculated and measured backscatter contributions. These small discrepancies are probably due to inaccuracies of the MC simulated model. As mentioned earlier, simulated energy deposition in the air of the BMC was used to compare with the reading by physical chamber. Therefore, no correction factors were taken into account for the calculated data as a potential source of error. Furthermore, some accurate details of Linac head are not available from manufacturer. For example, full geometrical details of the shielding ring around the beam transmit direction were not known that can influence the fluences of backscattered particles. However, we used the maximum available details of the BMC from the manufacturer as well as the Duzenli *et al.* (1993) study[12]. But, small error to simulate its detailed components (especially in the exit window) can change the reading of low energy backscattered particles.

Changes of the BMC response with removing the flattening filter (FFF mode)

Our calculated results for the FFF and FF modes for 6 MV photon beam are shown in Fig. 6a. Compared to the FF mode, the results for the FFF mode showed a systematic increase of approximately 0.6 % in the chamber response. This increase was not significant because of higher uncertainties. Therefore, removing the flattening filter from the Linac in 6 MV energy did not significantly change the chamber response.

The difference of the chamber response for 18 MV is significant for small field sizes (Fig. 6b). For example, at 0.5 × 0.5 cm^2 field size an increase of about 2.8 % in the chamber response was observed when the flattening filter removed. Increase in the backscattered particles, especially electrons, into the BMC from components located at the downstream surface of the chamber (upper and lower jaws and shielding rings) is due to this increase. In general, this difference is insignificant for the field sizes larger than 3 × 3 cm^2 that varied within the statistical uncertainties.

Spectra of forward directed and backscattered particles into the BMC

The spectra for 6 and 18 MV in the upstream plane of the BMC for forward directed photons and electrons for each field size and in the downstream plane of the BMC for the backscattered photons and electrons for the 0.5 × 0.5 cm^2 are shown in the Figs. 7 and 8.

The mean statistical uncertainties of the simulated spectra of the forward directed and backscattered photons and electrons for 6 MV and 18 MV are presented in Table 1.

Increasing the applied energy increases the fluences of the forward directed and backscattered particles reaching the BMC for both FF and FFF modes (Figs 6 & 7; Table 1). Decreasing the field size increases the backscatter fluences. Furthermore, removing the flattening filter increases the particles fluences. The increase in total fluence for the forward directed photons and electrons was 35.11 %, 116.06 % and 20.05 %, 10.09 % for 6 MV and 18 MV, respectively. The increase in total fluence for the backscattered photons and electrons was respectively 53.00 %, 61.68 % and

38.04 %, 38.35 % for 6 MV and 18 MV in the field size of 0.5 × 0.5 cm^2. The increase for the field size of 40 × 40 cm^2 was 46.67 %, 96.88 % and 25.23%, 22.87% for 6 MV and 18 MV, respectively. These increases can be attributed to the attenuation of the forward directed photon fluence and band the transferred or contaminating electrons from the target by the flattening filter. However, the flattening filter with low atomic number (made of copper, ^{29}Cu, and iron, ^{26}Fe, for 6 and 18 MV, respectively) acts as an electron producing source under FF mode, whereas eliminating the banding role against the electrons probably has more effective affect to increase electron fluences for the FFF mode.

The backscattered radiations have significantly lower average energies compared to the forward particles for both the FF and FFF modes of 6 MV or 18 MV (Table 1). For example, the average energy for the FF mode and 6 MV is 1.39 MeV and 0.36 MeV for the forward and backscattered photons and 1.08 MeV and 0.68 MeV for the forward and backscattered electrons for the field size of 0.5 × 0.5 cm^2. However, changing the field size does not change the average energies of the forward particles whereas increasing the field size decreases the average energy of the backscattered photons and electrons to 0.30 MeV and 0.47 MeV for the largest field size (40 × 40 cm^2), respectively. In the FF mode (6 MV) and 0.5 × 0.5 cm^2 field size, the average energy of 1.3 MeV and 0.3 MeV for the forward and backscattered photons, 1.2 MeV and 0.7 MeV for the forward and backscattered electrons, reported by Verhaegen *et al.* (2000) (9) is in good agreement with our data (Table 1).

Furthermore, removing the flattening filter reduces the average energy of particles. Removing the flattening filter decreases average energy of the forward directed photons and electrons by 2.88 %, 1.85 % and 1.89 %, 3.72 % for 6 MV and 18 MV, respectively. The average reduction of energy of the backscattered photons and electrons was 5.56 %, 5.88 % and 1.89 % and 0.75 % for 6 MV and 18 MV for the field size of 0.5 × 0.5 cm^2, respectively. The reduction value for the field size of 40 × 40 cm^2 was 6.67 %, 0 % and 5.26%, 6.32 % for 6 MV and 18 MV, respectively. For the FFF mode, removing the hardening effect (on the photon beam) and the banding effect (on the electron beam) shifted the average energy of the particles to the lower values.

Running separate simulations using surface sources that separately scored backscattered particles, the contribution of backscattered photons or electrons to the energy deposited in the chamber were calculated. However, the total amount of the backscattered photons reached into the downstream surface of chamber is higher than the backscattered electrons (Figs 6b, 7b) for both applied energies and modes but the ratio of mean contribution value of the backscattered photons in the total backscatter deposited energy, averaged over all the considered fields, was about 5 %. According to these results, the contribution from backscattered photons to the energy deposition in the BMC is very low that can be ignored and the energy deposition from backscatter radiations is mainly caused by backscattered electrons. Our results are consistent with the findings of Verhaegen *et al.* (2000)[9]. As mentioned in several studies, using a backscatter plate with appropriate thickness that is positioned after the chamber, it is possible to minimize the backscatter radiation effect[1, 12]. Our calculated results and spectra may be useful for such an effort.

CONCLUSION

The Monte Carlo simulations showed that increase of backscatter radiation into the BMC due to the decrease of field size is caused mainly by backscattered electrons. The calculated spectra may be useful to design appropriate material with desired thickness of backscatter plate to minimize the backscatter effect on BMC performance.

Our data indicate that removing the flattening filter does not change the BMC performance, compared with the conventional Linac with a flattening filter. However, this result is not valid for very smaller fields (e.g. 0.5 × 0.5 cm^2) of 18 MV beam thus corrected backscatter factors will be necessary to take into account the contribution of backscattered radiation into the BMC response in the case of free flattening filter mode.

ACKNOWLEDGMENT

This work was supported by Ahvaz Jundishahpur University of Medical Sciences [grant number U-89240].

REFERENCES

1. Hounsell AR. Monitor chamber backscatter for intensity modulated radiation therapy using multileaf collimators. *Physics in medicine and biology.* 1998; **43**(2):445-54. PubMed PMID: 9547177. eng.
2. Patterson MS, Shragge PC. Characteristics of an 18 MV photon beam from a Therac 20 Medical Linear Accelerator. *Med Phys*. 1981;**8**(3):312-8. PubMed PMID: 6798391. eng.
3. Luxton G, Astrahan MA. Output factor constituents of a high-energy photon beam. *Medical physics.* 1988;**15**(1):88-91. PubMed PMID: 3127668. eng.
4. Huang PH, Chu J, Bjarngard BE. The effect of collimator backscatter radiation on photon output of linear accelerators. *Medical physics.* 1987 ; **14**(2):268-9. PubMed PMID: 3587153. eng.
5. Yu MK, Sloboda RS, Mansour F. Measurement of photon beam backscatter from collimators to the beam monitor chamber using target-current-pulse-counting and telescope techniques. *Physics in medicine and biology.* 1996; **41**(7):1107-17. PubMed PMID: 8822779. eng.
6. Sharpe MB, Jaffray DA, Battista JJ, Munro P. Extrafocal radiation: a unified approach to the prediction of beam penumbra and output factors for megavoltage x-ray beams. *Medical physics.* 1995; **22**(12):2065-74. PubMed PMID: 8746712.
7. Watts DL, Ibbott GS. Measurement of beam current and evaluation of scatter production in an 18-MeV accelerator. *Medical physics.* 1987; **14**(4):662-4. PubMed PMID: 3627007.
8. Lam KL, Muthuswamy MS, Ten Haken RK. Measurement of backscatter to the monitor chamber of medical accelerators using target charge. *Medical physics.* 1998; **25**(3):334-8. PubMed PMID: 9547500. eng.
9. Verhaegen F, Symonds-Tayler R, Liu HH, Nahum AE. Backscatter towards the monitor ion chamber in high-energy photon and electron beams: charge integration versus Monte Carlo simulation. *Physics in medicine and biology.* 2000; **45**(11):3159-70. PubMed PMID: 11098896. eng.
10. Kubo H. Telescopic measurements of backscattered radiation from secondary collimator jaws to a beam monitor chamber using a pair of slits. *Medical physics.* 1989;**16**(2):295-8. PubMed PMID: 2497317.
11. Kubo H, Lo KK. Measurements of backscattered radiation from Therac-20 collimator and trimmer jaws into beam monitor chamber. *Medical physics.* 1989; **16**(2):292-4. PubMed PMID: 2497316. eng.
12. Duzenli C, McClean B, Field C. Backscatter into the beam monitor chamber: implications for dosimetry of asymmetric collimators. *Medical physics*. 1993; **20**(2 Pt 1):363-7. PubMed PMID: 8497223. eng.
13. Verhaegen F, Das IJ. Monte Carlo modelling of a virtual wedge. *Physics in medicine and biology.* 1999; **44**(12):N251-9. PubMed PMID: 10616157.
14. Jiang SB, Boyer AL, Ma CM. Modeling the extrafocal radiation and monitor chamber backscatter for photon beam dose calculation. *Medical physics.* 2001; **28**(1):55-66. PubMed PMID: 11213923. eng.
15. Vassiliev ON, Titt U, Kry SF, Ponisch F, Gillin MT, Mohan R. Monte Carlo study of photon fields from a flattening filter-free clinical accelerator. *Medical physics.* 2006; **33**(4):820-7. PubMed PMID: 16696457.
16. Vassiliev ON, Titt U, Ponisch F, Kry SF, Mohan R, Gillin MT. Dosimetric properties of photon beams from a flattening filter free clinical accelerator. *Physics in medicine and biology.* 2006; **7**;51(7):1907-17. PubMed PMID: 16552113.
17. Mesbahi A, Mehnati P, Keshtkar A, Farajollahi A. Dosimetric properties of a flattening filter-free 6-MV photon beam: a Monte Carlo study. *Radiat Med*. 2007; **25**(7):315-24. PubMed PMID: 17705000.
18. Vassiliev ON, Titt U, Kry SF, Mohan R, Gillin MT. Radiation safety survey on a flattening filter-free medical accelerator. *Radiat Prot Dosimetry.* 2007; **124**(2):187-90. PubMed PMID: 17681966.
19. Mesbahi A, Nejad FS. Monte Carlo study on a flattening filter-free 18-MV photon beam of a medical linear accelerator. *Radiat Med.* 2008; **26**(6):331-6. PubMed PMID: 18677606.
20. Vassiliev ON, Kry SF, Chang JY, Balter PA, Titt U, Mohan R. Stereotactic radiotherapy for lung cancer using a flattening filter free Clinac. *J Appl Clin Med Phys.* 2009; **10**(1):2880. PubMed PMID: 19223837.
21. Almond PR, Biggs PJ, Coursey BM, Hanson WF, Huq MS, Nath R, et al. AAPM's TG-51 protocol for clinical reference dosimetry of high-energy photon and electron beams. *Med Phys.* 1999; **26**(9):1847-70. PubMed PMID: 10505874. eng.
22. Walter LS. (Ed.) Monte Carlo N-Particle transport code system for multiparticle and high energy applications LANL (Los Alamos

National Laboratory), version 2.4.0, Ref Type: Serial (Book, Monograph). 2002.

23. Dubuque GL, Cacak RK, Hendee WR. Backscatter factors in the mammographic energy range. Medical physics. 1977 Sep-Oct;4(5):397-9. PubMed PMID: 904590. eng.
24. Ding GX. Dose discrepancies between Monte Carlo calculations and measurements in the buildup region for a high-energy photon beam. *Medical physics*. 2002; **29**(11):2459-63. PubMed PMID: 12462709. eng.
25. Abdel-Rahman W, Seuntjens JP, Verhaegen F, Deblois F, Podgorsak EB. Validation of Monte Carlo calculated surface doses for megavoltage photon beams. *Medical physics*. 2005; **32**(1):286-98. PubMed PMID: 15719980. eng.
26. Hartmann Siantar CL, Walling RS, Daly TP, Faddegon B, Albright N, Bergstrom P, et al. Description and dosimetric verification of the PEREGRINE Monte Carlo dose calculation system for photon beams incident on a water phantom. *Medical physics*. 2001; **28**(7):1322-37. PubMed PMID: 11488562. eng.
27. Nath R, Epp ER, Laughlin JS, Swanson WP, Bond VP. Neutronfromhigh-energy x-ray medical accelerators: Anestimate of risk to the radiotherapy patient. *Med Phys.* 1984; **11**: 231–41.